JOURNAL OF MATERIALS SCIENCE 27 (1992) 1818–1826

AES and SIMS investigations of the oxide films on Fe–40Cr–Ru alloys

S. C. TJONG
Department of Applied Science, City Polytechnic of Hong Kong, 83 Tat Chee Avenue, Kowloon, Hong Kong

W. O. BARNARD, J. B. MALHERBE
Department of Physics, University of Pretoria, Pretoria 0002, South Africa

Auger and SIMS depth profiling have been used to investigate the effect of ruthenium addition on the oxidation behaviour of the Fe–40Cr–Ru alloys oxidized in air at 500 °C. Auger results revealed that the oxide films formed on the Fe–40Cr–Ru alloys consisted of a thin iron oxide external layer and a chromium-rich internal layer. Ruthenium was not found in these oxide layers. Secondary ion mass spectrometry measurements also indicated a thin Fe^+-rich film as an outer layer with a predominantly chromium oxide in the internal layer of the film. Furthermore, ruthenium was incorporated in the entire oxide film and promoted the formation of a thin compact film.

1. Introduction

Previous work has demonstrated that the oxidation rate of iron-based alloys is reduced by the presence of chromium and palladium [1, 2]. Addition of chromium to the iron-based alloys at and above 9% leads to an initial formation of chromium oxide on the alloy surface at 500 °C. It is then followed by an oxide formation of the component with lower affinity for oxygen on top of the chromium oxide [2]. On the other hand, platinum group metal (PGM) additions, especially palladium have been shown to promote the formation of chromium oxide on the iron-based alloys at 550 °C as palladium is completely oxidized before the oxidation of chromium begins and this PdO offers easy diffusion paths for chromium [3, 4]. From an economic view point, it is advantageous to use lower cost ruthenium as an alloying element rather than palladium, provided that ruthenium also enhances the formation of the chromium oxide. More recently, van Staden and Roux [5] reported that ruthenium restrains the formation of iron oxides and promotes the formation of chromium oxide due to the preferential segregation of chromium.

The development of surface analytical techniques, such as Auger electron spectroscopy (AES), X-ray photoelectron spectroscopy (XPS) and secondary ion mass spectrometry (SIMS) has facilitated the investigation of the oxide films formed on the Fe–Cr alloys [1–15]. Each of these techniques has its own shortcomings and they are complementary to each other. A combination of two or more surface techniques have enhanced our understanding of the oxidation behaviour of the Fe–Cr alloys [8, 10]. SIMS is extremely surface-sensitive compared to Auger or XPS, and the detection limit attains a range from parts per million to parts per billion. The detection sensitivity of elements with SIMS is more affected by changes in the matrix than that of the Auger and XPS. Furthermore, the secondary ion intensity can be markedly increased by bombarding the sample with oxygen primary ions [16, 17]. SIMS has several modes of operation, i.e. static, dynamic and imaging. In the static mode, low-energy low-flux primary ions are bombarded on to a relatively large target area, and the secondary ions emitted are mass-separated and detected. The static SIMS, in principle, is sensitive to only one or at most two atomic layers, and this method has been used to investigate the surface oxidation of chromium [18]. Dynamic SIMS employs a high primary ion current density to obtain a very high yield of secondary ions. The depth profile is obtained by measuring the secondary ion signal as a function of the sputter time. The aim of the present work was to characterize the oxide film formed on the Fe–40Cr–Ru alloys at 500 °C by means of Auger and SIMS techniques. SIMS was particularly useful in the present study because it can detect the presence of small amounts of ruthenium in the oxide films, whereas with the AES the strongest Auger peak for Ru (273 eV) tends to overlap with the principal peak for C(272 eV).

2. Experimental procedure

The Fe–40Cr–0.4Ru, Fe–40Cr–1Ru and Fe–40Cr–3Ru alloys were prepared by vacuum induction melting and they were subsequently cast into ingots. The chemical compositions of the alloys investigated are tabulated in Table I. Disc specimens of 11 mm diameter and 2 mm thickness were cut from these ingots. They were solution annealed at 1200 °C for 2 h, followed by quenching in water. One side of each disc was mechanically ground with a series of decreasing

0022–2461

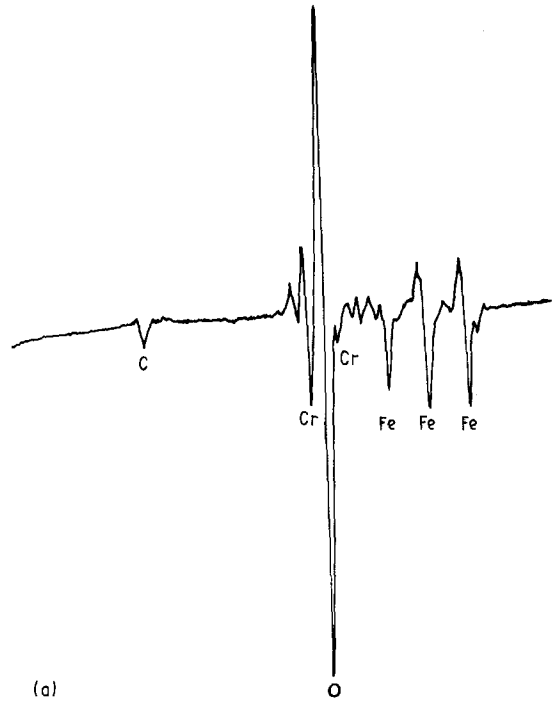

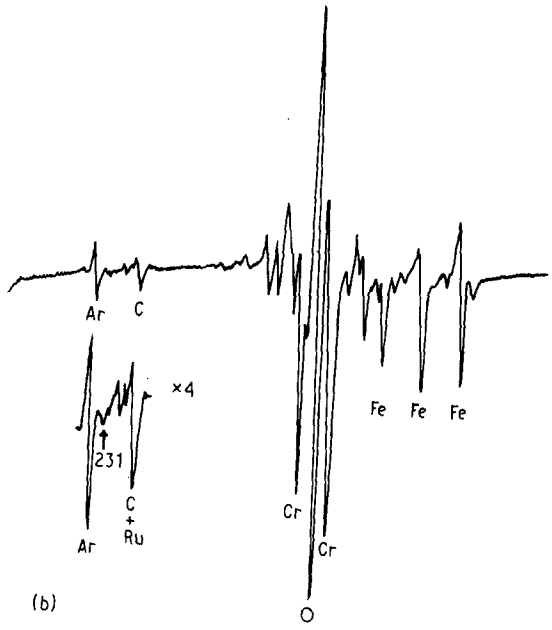

Figure 1 Auger spectra of the oxide film formed on the Fe–40Cr–3Ru alloy in air at 500 °C. (a) Before sputtering, (b) after sputtering for 33 min, (c) Auger spectrum of the clean Fe–40Cr–3Ru substrate alloy.

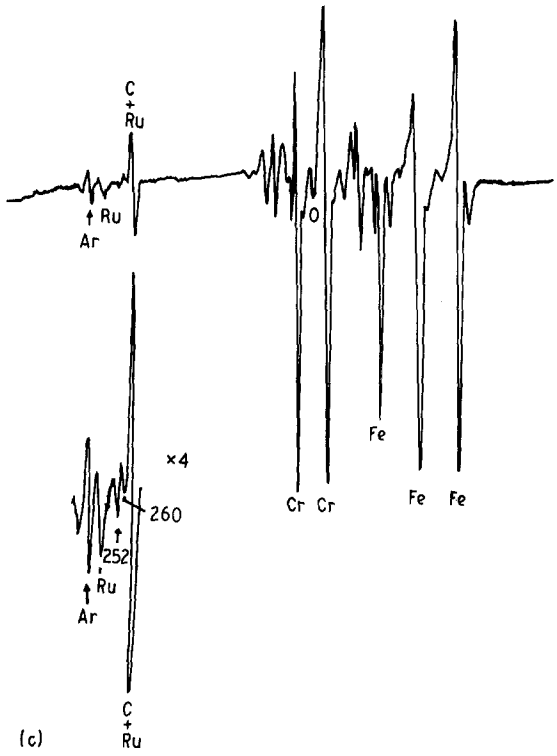

grit sizes, the final polish being with 1 μm diamond paste. The specimens were ultrasonically cleaned in distilled water, dried and subsequently oxidized in air at 500 °C for 2 h. After oxidation, the specimens were removed from the furnace, cooled to room temperature and transferred into ultra-high vacuum (UHV) chambers of the Auger and SIMS spectrometers.

TABLE I Chemical compositions of the alloys investigated (wt %)

Alloy	C	S	N	Cr	Ru	Fe
Fe–40Cr–0.4Ru	0.01	0.01	0.004	38.9	0.41	Bal.
Fe–40Cr–1Ru	0.02	0.01	0.003	40.5	0.90	Bal.
Fe–40Cr–3Ru	0.02	0.01	0.005	39.4	3.0	Bal.

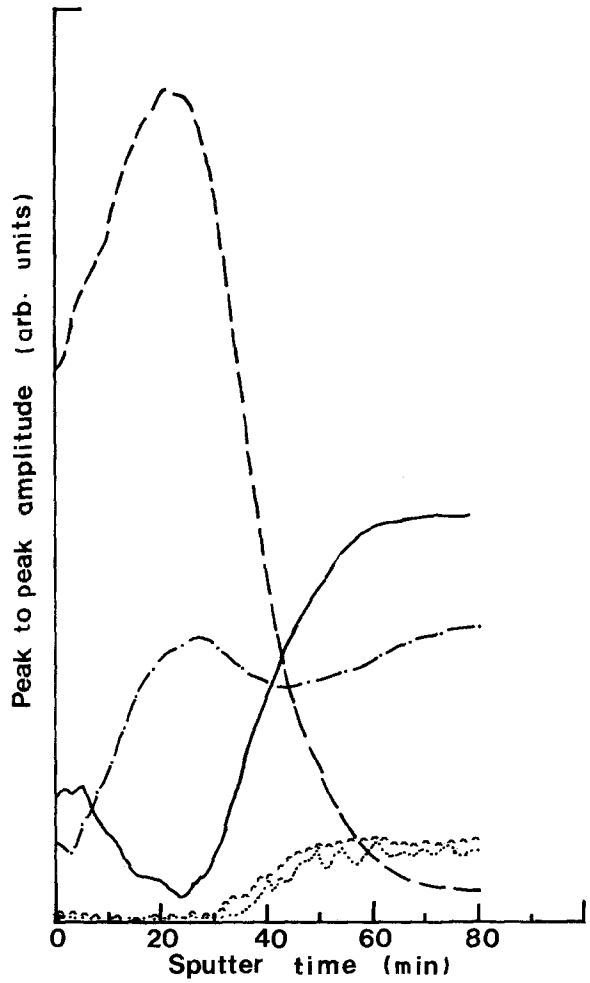

Figure 2 Auger depth profile of the oxide film formed on the Fe–40Cr–3Ru alloy in air at 500 °C. (– – –) Oxygen, (——) iron, (— · —) chromium, (· · ·) ruthenium, × 5, (^ ^ ^) carbon.

The Auger measurements were made with a Varian UHV chamber equipped with a Physical Electronics Industries model 15-110A single-pass cylindrical mirror analyser. A primary electron beam energy of 5 keV and current of 2 μA was used for excitation. Depth profiles were obtained by sputtering the oxide films with an argon beam of an energy of 2 keV, a current density of 7 $\mu A\,cm^{-2}$ and a pressure of 3.5×10^{-5} torr (1 torr = 1.333×10^2 Pa). The sputter rate was about 0.4 $nm\,min^{-1}$ based on a Ta_2O_5 film of known thickness. For each profile, the peak-to-peak heights (p.p.h.) for Ru(231 eV), C(272 eV), O(509 eV) and Fe(701 eV) were monitored automatically with a multiplexer and a point plotter. The negative going peak height of the Cr(529 eV) was monitored due to the interference of the Cr(529 eV) peak with the O(510 eV) peak [1]. The Ru(231 eV) was used because the strongest peak for Ru(273 eV) overlaps with the C(272 eV) peak.

SIMS analyses were carried out in a quadrupole-based SIMSLAB attached to the VG ESCALAB MK II spectrometer. The analyses were performed with a gallium liquid-metal ion source operated at 10 keV, beam current of 3 nA and a pressure of 3.36×10^{-10} torr. The ion beam was rastered over an area of about 280 μm × 340 μm. The signal was gated so that the data were collected over a small area located centrally.

3. Results and discussion

Fig. 1a and b show typical Auger spectra of the oxide film formed on the Fe–40Cr–3Ru alloy before sputtering and after sputtering for 33 min, whereas the Auger spectrum of the clean Fe–40Cr–3Ru alloy is shown in Fig. 1c. The spectra reveal that ruthenium was not initially present in the surface oxide film, and only begins to appear in the oxide film after sputtering for ~ 33 min, as seen by the presence of a very small peak located at 231 eV (Fig. 1b). Looking at the substrate alloy, the intensity of the Ru(231 eV) peak increases dramatically. The Auger spectrum of the substrate alloy clearly reveals the formation of chromium carbides on the basis of Auger peaks located at 250, 260 and 271 eV which overlaps with ruthenium peak [19]. The Auger depth profile of the oxide film formed on the Fe–40Cr–3Ru alloy at 500 °C is shown in Fig. 2. The thickness of the oxide film

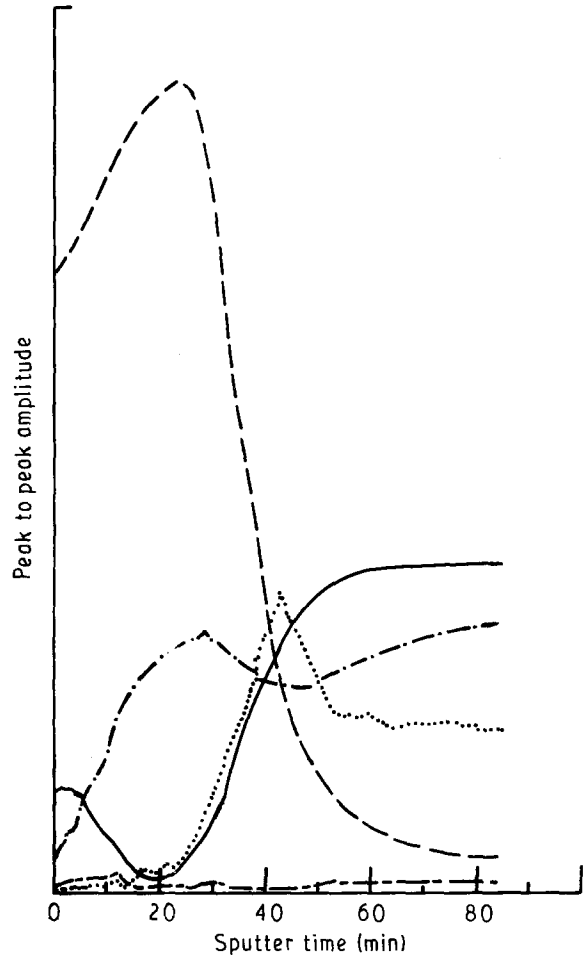

Figure 3 Auger depth profile of the oxide film formed on the Fe–40Cr–3Pd alloy in air at 500 °C [2]. (– – –) Oxygen, (——) iron, (—·—) chromium, (···) palladium, × 5, (—·—·—) carbon.

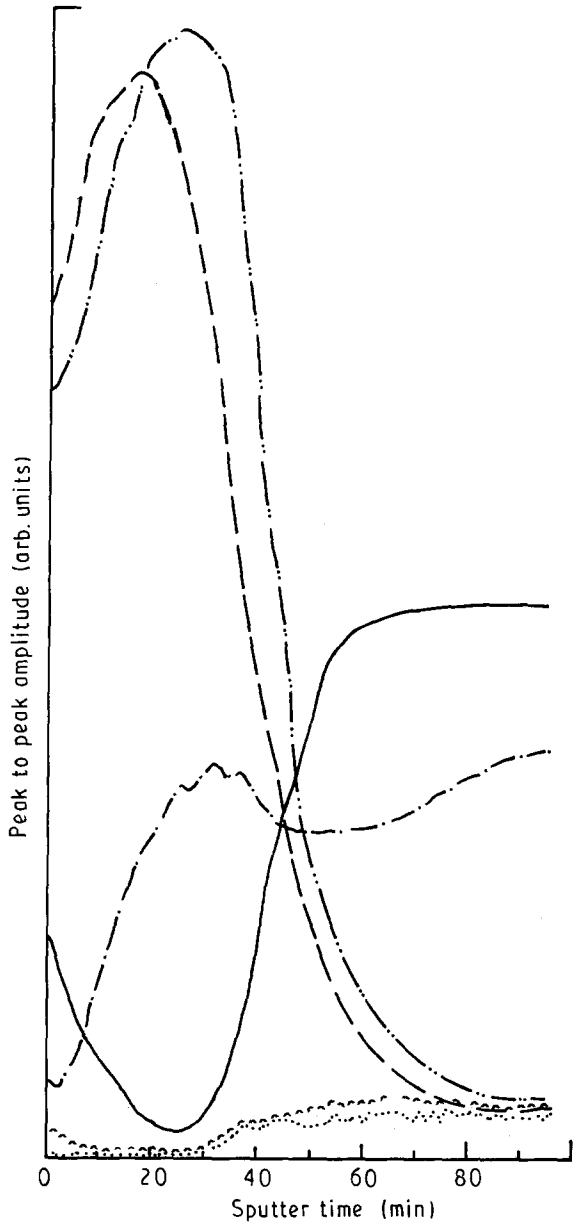

Figure 4 Auger depth profile of the oxide film formed on the Fe–40Cr–1Ru alloy in air at 500 °C. The oxygen profile of the oxidized Fe–40Cr–0.4Ru alloy is also shown for the purpose of comparison. (—···—) Oxygen (0.4Ru), (– – –) oxygen, (——) iron, (—·—·—) chromium, (···) ruthenium, × 5, (^^^) carbon.

formed on this alloy was estimated at approximately 16 nm from the oxygen signal at half of its maximum amplitude. The oxide structure formed on this alloy in general is similar to that formed on other Fe–Cr alloys, as reported previously, i.e. innermost chromium oxide next to the substrate alloy, intermediate $Fe_{3-x}Cr_xO_4$ and outermost Fe_2O_3 [1]. This surface composition depends greatly on the selective surface reaction and diffusion rates of various cations through the reacting film. Thus chromium was initially selectively oxidized because of its large affinity for oxygen and the large negative free energy of formation of the chromium oxide. However, because of the larger mobility of the Fe^{3+} cations [15], they diffused through the chromium oxide layer and this resulted in the formation of the spinel $Fe_{3-x}Cr_xO_4$. On further oxidation, an outermost α-Fe_2O_3 layer was formed.

From Fig. 2, it is apparent that ruthenium is detected near the oxide–alloy interface but is not enriched near this region. Furthermore, the carbon signal associated with the chromium carbides increases near the substrate alloy due to the contribution from the Ru(273 eV) peak. For the purpose of comparison, the AES depth profile of the oxide film formed on the Fe–40Cr–3Pd alloy at 500 °C is shown in Fig. 3 [2]. It can be seen that a PdO-enriched layer exists between the oxide layer and the substrate alloy, and this PdO layer provides easy diffusion paths for chromium. Fig. 4 shows the AES depth profile of the oxide film formed on the Fe–40Cr–1Ru alloy at 500 °C. The thickness of the oxide film is approximately 16.1 nm. This AES depth profile shows similar features to that of the Fe–40Cr–3Ru alloy. The oxygen profile of the oxide film formed on the Fe–40Cr–0.4Ru alloy is also shown in Fig. 4. The thickness of the oxide film on the Fe–40Cr–0.4Ru alloy is approximately 18 nm. Thus addition of 1% Ru to the Fe–40Cr alloy is sufficient to promote the formation of a compact film. From the Auger studies done by van Staden and Roux [5, 20], it was reported that no surface segregation of ruthenium occurred in the Fe–40Cr–3Ru alloy at temperatures below 600 °C in contrast with the palladium surface segregation. However, strong preferred segregation of chromium with respect to iron was observed between 400 and 500 °C. A strong chromium enrichment at the surface at temperatures above 275 °C in a controlled oxygen atmosphere, is possibly due to an attractive interaction between ruthenium and iron in the bulk [5].

Fig. 5a and b show SIMS Fe^+, Cr^+, FeO^+ and CrO^+ peak heights as a function of depth into the oxide film formed on the Fe–40Cr–0.4Ru alloy at 500 °C. The Cr^+ signal shows a sharp decrease at the outermost surface region, followed by a plateau region and decreases again near the oxide–substrate interface. This is expected due to the fact that the secondary ion yield (M^+) of the metallic oxides is higher than

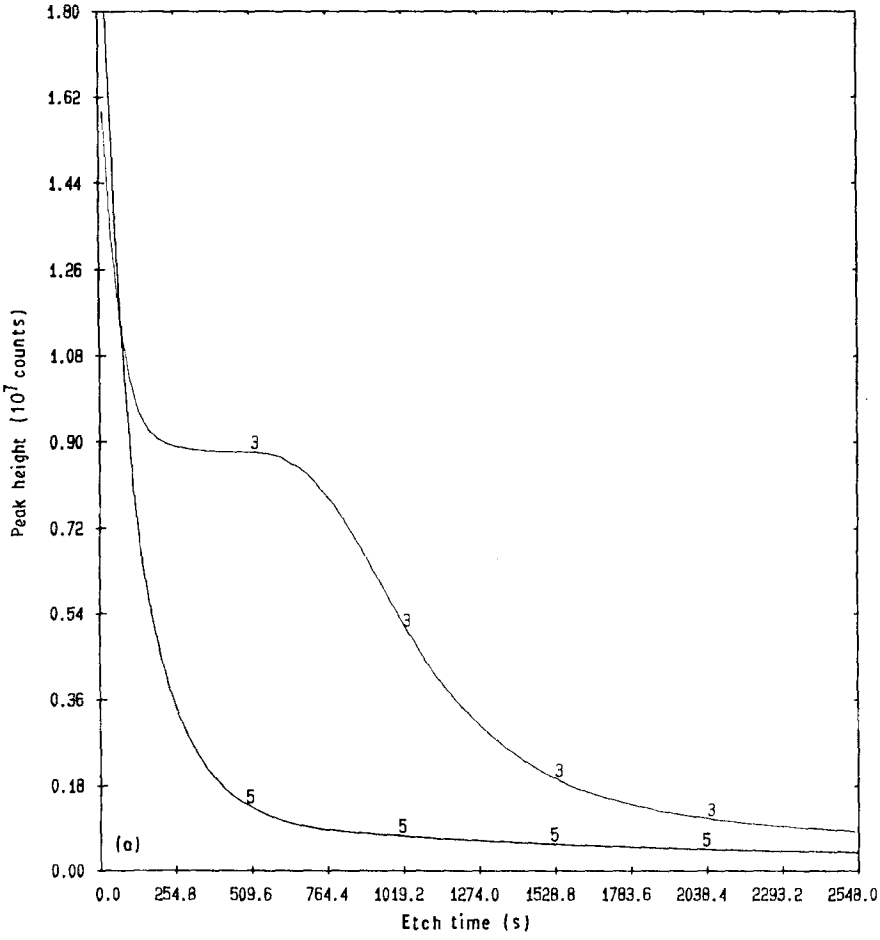

Figure 5 SIMS sputter profiles for the Fe–40Cr–0.4Ru alloy oxidized in air at 500 °C (a) 3 and 5 indicate Cr^+ and Fe^+ curves, respectively; (b) 4 and 6 indicate CrO^+ and FeO^+ curves, respectively; (c) 1 and 2 indicate Ru^+ and RuO^+ curves, respectively.

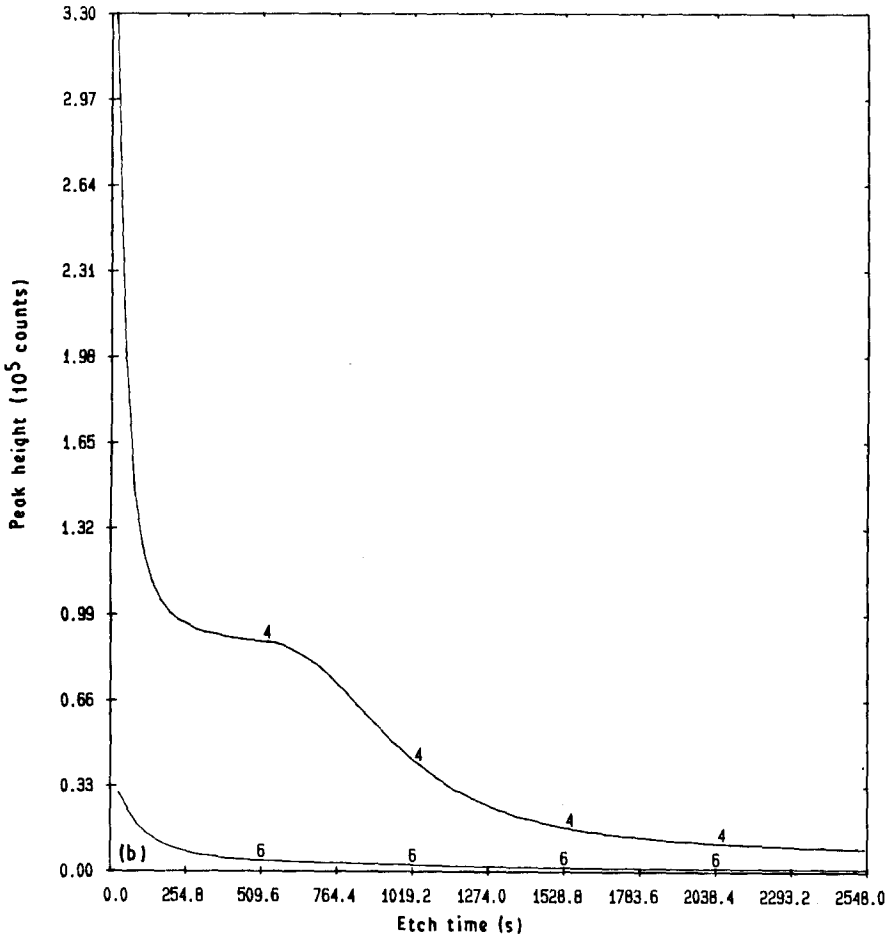

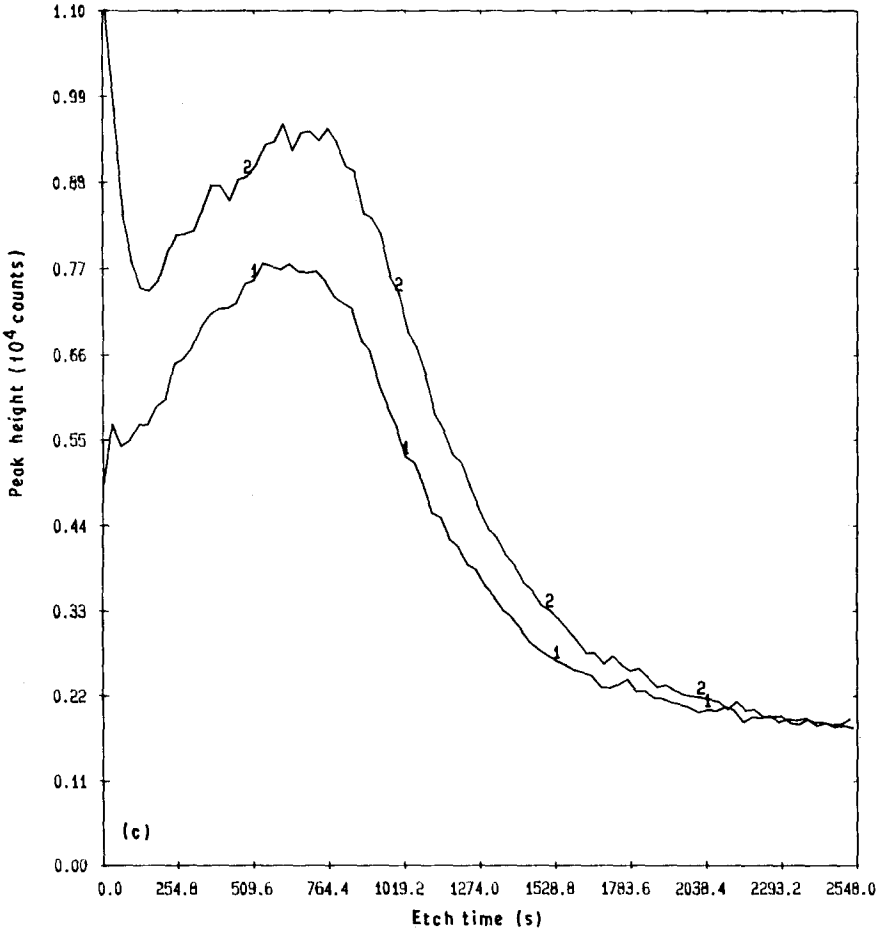

Figure 5 Continued.

that of the pure metal [21]. Moreover, this behaviour is also likely to be associated with a change in the sputtering rate of chromium within the oxide layers and the substrate. The Fe^+ and FeO^+ profiles indicate that the iron oxide was formed only at the outermost oxide region, and this is in agreement with the Auger results which show that a thin external α-Fe_2O_3 layer was formed on the Fe–Cr alloys during oxidation at 500 °C [1]. On the other hand, ruthenium was observed to be incorporated into the entire oxide film and shows an apparent maximum within the film on the basis of the Ru^+ and RuO^+ profiles as shown in Fig. 5c. Thus SIMS observations provide useful information on the distribution and movement of ruthenium in the oxide film formed on the Fe–40Cr–0.4Ru alloy while Auger depth profiles shows an absence of ruthenium in the oxide films formed on the Fe–40Cr–Ru alloys containing up to 3%. According to the literature, a thin protective RuO_2 oxide film was formed on the pure ruthenium between 327 and 677 °C [22]. Previous XPS studies indicated that ruthenium tends to be incorporated in the oxide films formed on the Fe–40Cr–(0.1–0.2)Ru alloy exposed in the sulphuric and hydrochloric acid solutions as Ru^{4+} species [23, 24]. The incorporation of the Ru^{4+} species in a hydrated chromium-rich film promotes the spontaneous passivation of the Fe–40Cr–(0.1–0.2)Ru alloys and hence increasing the corrosion resistance of these alloys in the reducing acids [23, 24]. From SIMS results, it is suggested that Cr^{3+} and Ru^{4+} cations diffused out from the bulk alloy and reacted with the oxygen anions in forming a chromium-rich ruthenium-containing oxide layer. Fe^{3+} cations later diffused through vacant lattice positions of this oxide layer to the oxide–gas interface and reacted with oxygen anions to form a thin α-Fe_2O_3 layer.

Fig. 6a–c show SIMS Fe^+, Cr^+, FeO^+, CrO^+, Ru^+ and RuO^+ peak heights as a function of depth for the Fe–40Cr–1Ru alloy oxidized in air at 500 °C. These profiles exhibit similar characteristics as those for the Fe–40Cr–0.4Ru alloys shown in Fig. 5a–c. However, it is noted that the sputtering time required to remove the CrO^+ and RuO^+ on the Fe–40Cr–1Ru alloy is approximately 1990 s, which is slightly shorter than that for the Fe–40Cr–0.4Ru alloy ($\sim$ 2293 s). For the Fe–40Cr–3Ru alloy, the time needed to sputter the CrO^+ and RuO^+ is even shorter, i.e. 1244 s (Fig. 7a and b). Thus ruthenium alloying facilitates the formation of a thinner oxide film.

4. Conclusion

The Auger depth profiles reveal that ruthenium was absent in the oxide films formed on the Fe–40Cr–Ru alloys at 500 °C. However, SIMS sputter depth profiles indicate that ruthenium was incorporated into the chromium oxide formed on these alloys at 500 °C,

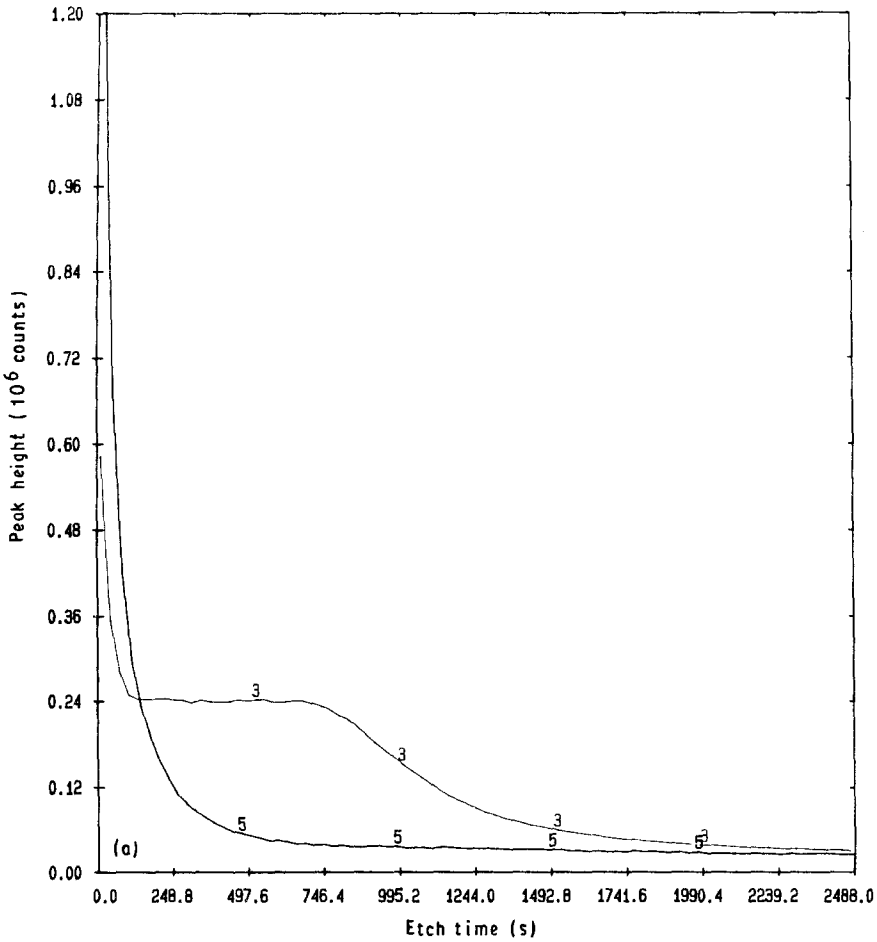

Figure 6 SIMS sputter profiles for the Fe–40Cr–1Ru alloy oxidized in air at 500 °C. (a) 3 and 5 indicate Cr^+ and Fe^+ curves, respectively; (b) 4 and 6 indicate CrO^+ and FeO^+ curves, respectively; (c) 1 and 2 indicate Ru^+ and RuO^+ curves, respectively.

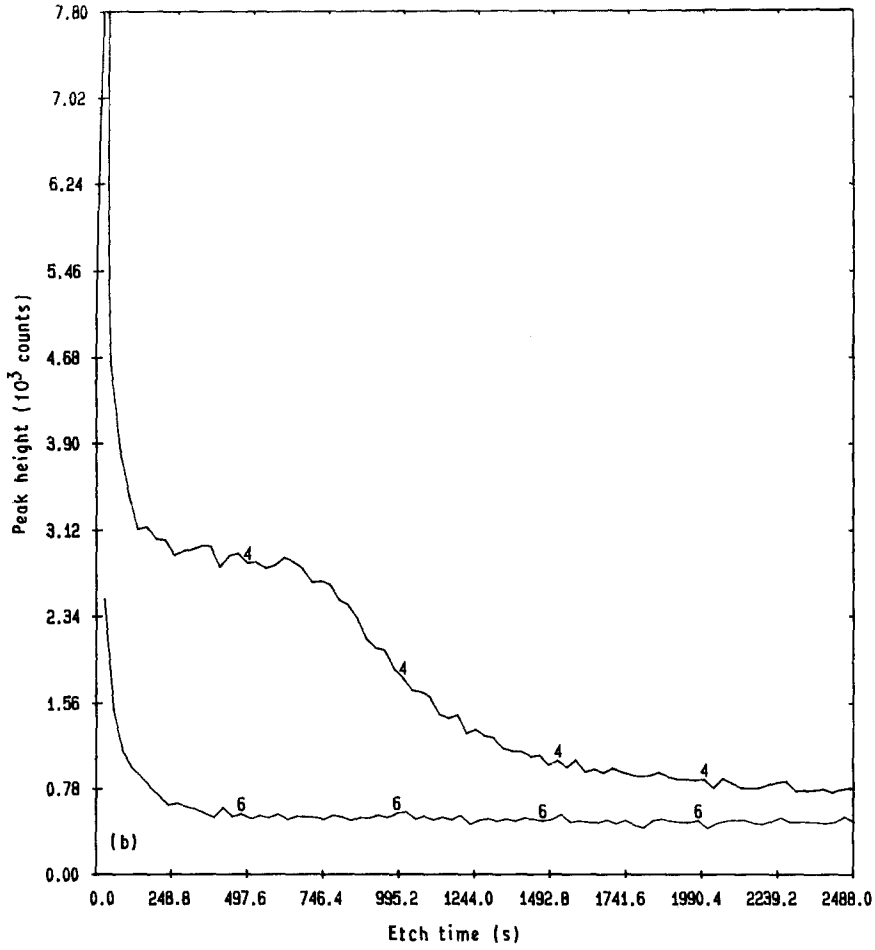

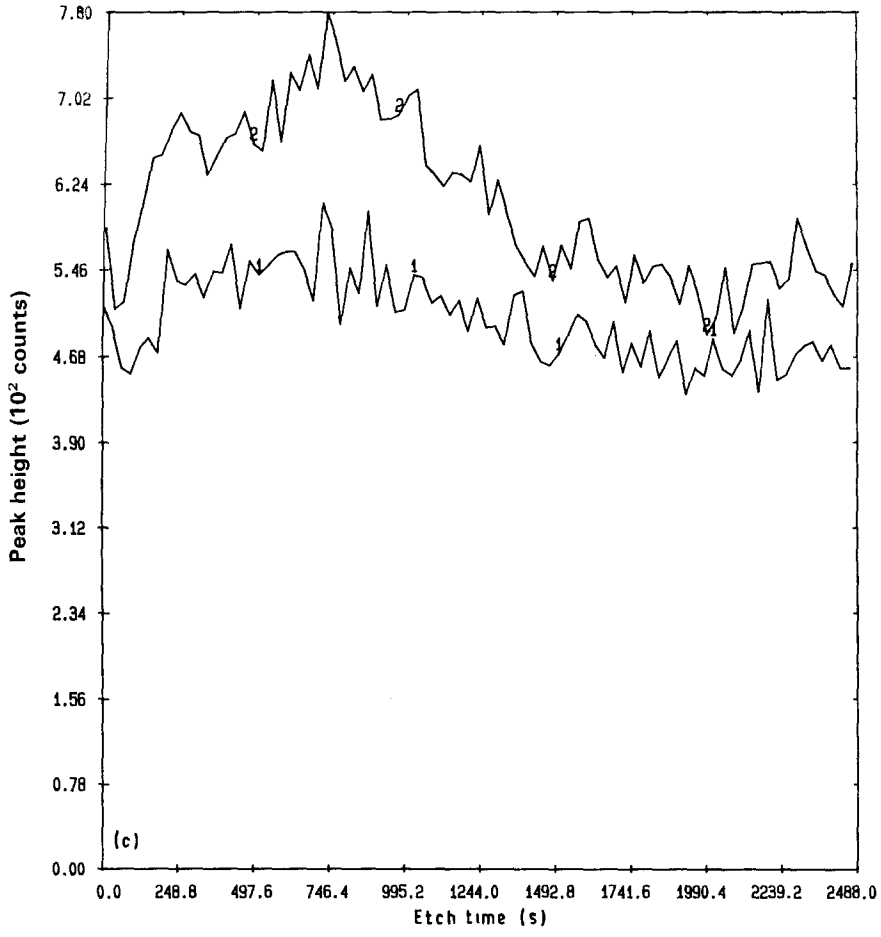

Figure 6 Continued.

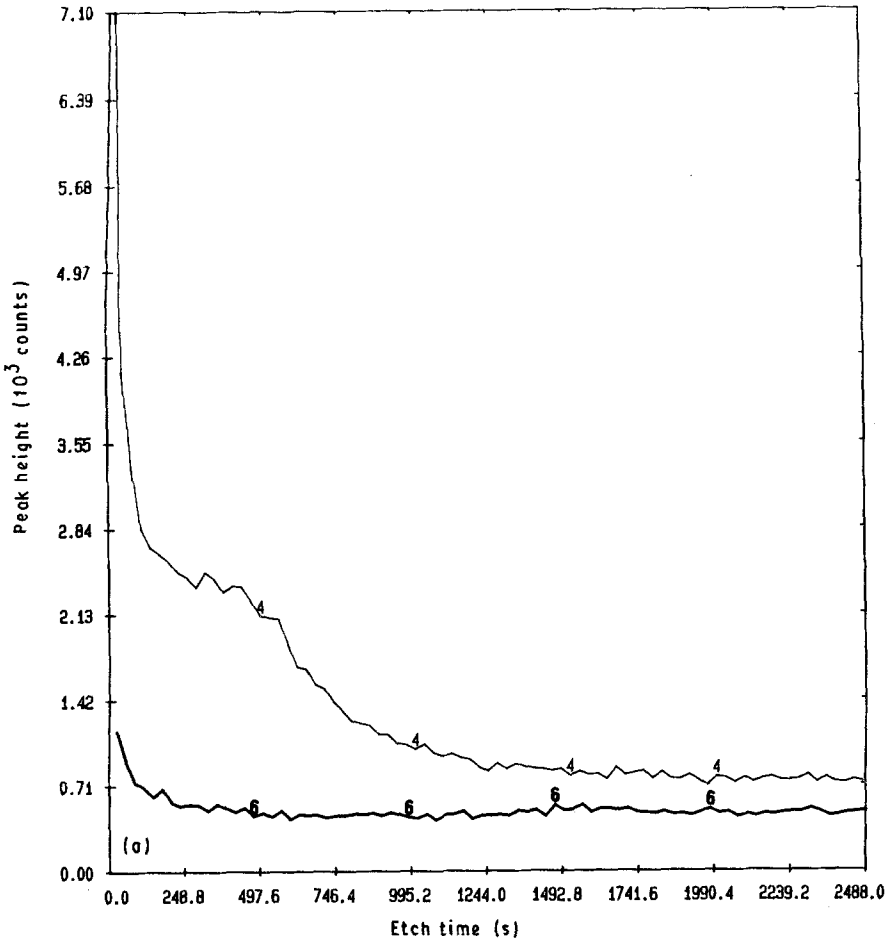

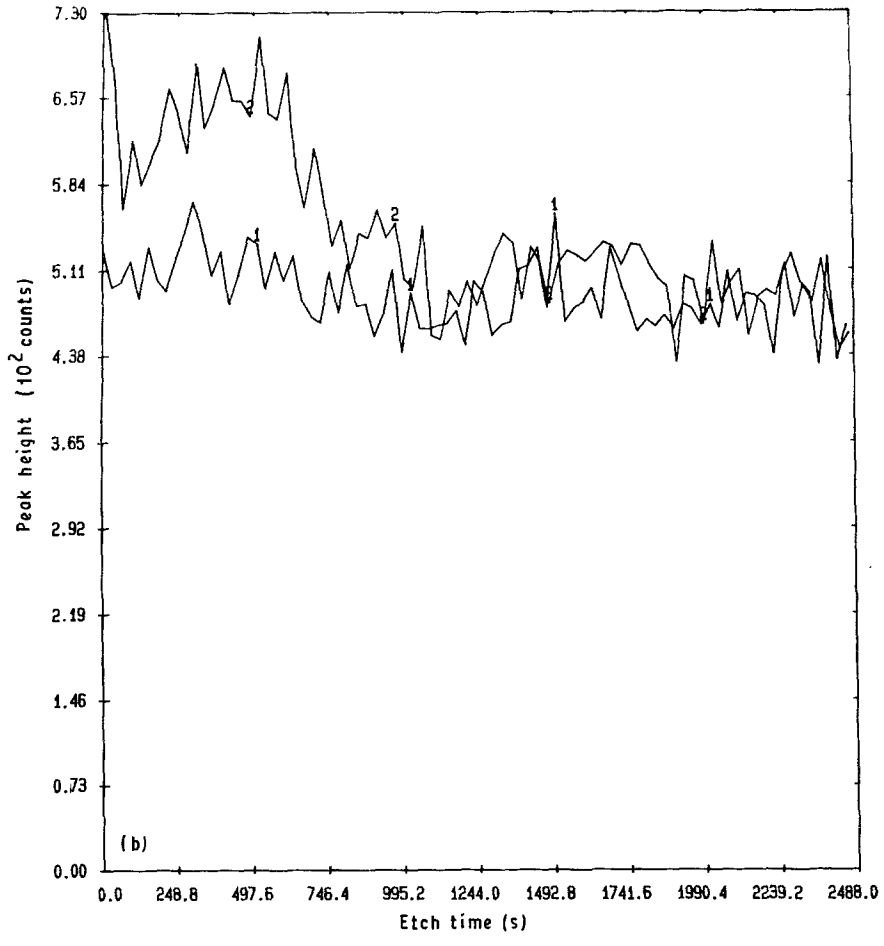

Figure 7 SIMS sputter profiles for the Fe–40Cr–3Ru alloy oxidized in air at 500 °C. (a) 4 and 6 indicate CrO^+ and FeO^+ curves, respectively; (b) 1 and 2 indicate Ru^+ and RuO^+ curves, respectively.

and ruthenium promotes the formation of a thinner oxide film.

References

1. S. C. TJONG, J. ELDRIDGE and R. W. HOFFMAN, *Appl. Surf. Sci.* **14** (1982–83) 297.
2. S. C. TJONG and J. B. MALHERBE, *ibid.* **40** (1989) 1.
3. W. E. DELPORT and J. P. ROUX, *Corros. Sci.* **26** (1986) 407.
4. D. J. HOLTZHAUSEN and J. P. ROUX, *ibid.* **30** (1990) 67.
5. M. J. van STADEN and J. P. ROUX, *Appl. Surf. Sci.* **44** (1990) 263.
6. P. J. OSBORNE and P. J. K. PATERSON, *ibid.* **15** (1983) 66.
7. W. L. N. MATTHEWS, P. J. K. PATERSON and H. K. WAGENFELD, *ibid.* **15** (1983) 281.
8. H. J. MATTHIEU and D. LANDOLT, *Corros. Sci.* **26** (1986) 547.
9. D. R. BAER, *Appl. Surf. Sci.* **7** (1981) 69.
10. G. R. CONNER, in "Applied Surface Analysis", ASTM STP 699, edited by T. L. Barr and L. E. Davies (American Society for Testing and Materials, Philadelphia, PA 1980) pp. 54–65.
11. I. OLEFJORD, *Corros. Sci.* **15** (1975) 687.
12. K. ASAMI, H. HASHIMOTO and S. SHIMODAIRA, *ibid.* **18** (1978) 125.
13. C. J. GREYLING and J. P. ROUX, *ibid.* **24** (1984) 675.
14. T. TANABE and S. IMOTO, *Trans. Jpn. Inst. Met.* **20** (1979) 507.
15. G. C. ALLEN, J. M. DYKE, S. J. HARRIS and A. MORRIS, *Oxid. Met.* **29** (1988) 391.
16. C. A. ANDERSEN, *Int. J. Mass Spectrom. Ion Phys.* **2** (1969) 61.
17. *Idem., ibid.* **3** (1970) 413.
18. A. BENINGHOVEN and A. MULLER, *Surf. Sci.* **39** (1973) 416.
19. L. E. DAVIS, N. C. MacDONALD, P. W. PALMBERG, G. E. RIACH and R. E. WEBER, "Handbook of Auger Electron Spectroscopy", 2nd Edn (Physical Electronics Industries, Eden Prairie, MN, 1976) p. 29.
20. M. J. VAN STADEN and J. P. ROUX, *Appl. Surf. Sci.* **44** (1990) 271.
21. A. BENINGHOVEN, in "Chemistry and Physics of Solid Surfaces", edited by R. Vanselow and S. Y. Tong (CRC Press, Cleveland, OH, 1977) p. 207.
22. G. K. L. CRANSTOUN, D. R. PYKE and G. D. W. SMITH, *Appl. Surf. Sci.* **2** (1979) 375.
23. S. C. TJONG, *ibid.* **44** (1990) 7.
24. *Idem., ibid.* **45** (1990) 301.

Received 26 November 1990
and accepted 10 April 1991